Onset of oscillatory binary fluid convection in finite containers

Oriol Batiste,[1] Isabel Mercader,[1] Marta Net,[1] and Edgar Knobloch[2]
[1]*Departament de Física Aplicada, Universitat Politècnica de Catalunya, Barcelona, Spain*
[2]*Department of Physics, University of California at Berkeley, Berkeley, California 94720*
(Received 22 December 1998)

The onset of oscillatory convection in binary fluid mixtures in a two-dimensional domain with realistic boundary conditions on all boundaries is determined as a function of the fluid parameters and the aspect ratio Γ of the container. The first unstable mode has either odd or even parity under left-right reflection. Depending on Γ and the separation ratio S, this mode has the form of a standing wave, or a ''chevron,'' consisting of a pair of waves propagating outwards from the cell center (or, in some cases, inwards towards it). Codimension-two points at which odd and even parity modes are simultaneously marginally stable are determined, as are various Takens-Bogdanov points. For fixed $S<S_{TB}$, all mode interactions among modes of like parity, arising as Γ varies, are of the nonresonant Hopf-Hopf type; however, the details of the modal interchange are organized by resonant Hopf bifurcations with 1:1 resonance. Particular attention is paid to the asymptotic mode structure as $\Gamma\to\infty$, and to the gap (in Rayleigh number and oscillation frequency) between successively unstable modes. The results quantify the parameter regime in which the weakly nonlinear dynamics of the system can be described in terms of the interaction of the first odd and even parity oscillatory modes.
[S1063-651X(99)06706-9]

PACS number(s): 47.20.Bp, 47.20.Ky, 47.27.Te, 41.20.Jb

I. INTRODUCTION

Binary fluid mixtures with a negative separation ratio exhibit a wide variety of behavior when heated from below. Particular attention has focused on the transition to various types of traveling waves with increasing Rayleigh number. The experimental situation is summarized in Refs. [1,2]. Some of these experiments have been carried out in narrow gap annular containers, others in rectangular boxes. The two experimental arrangements differ in a fundamental way. In the former, the system is periodic and consequently the initial instability can develop into a uniform pattern of traveling waves. This is no longer so when sidewalls are present. The presence of sidewalls destroys the translation invariance present in the annular (or unbounded) system, with the result that the finite system has only a left-right reflection symmetry. Consequently, the eigenfunctions of the latter system are either odd or even under left-right reflection, but are otherwise unconstrained by the symmetries [3]. In contrast, in the annular (or unbounded) case the presence of translation invariance with periodic boundary conditions forces the eigenfunctions to be sinusoidal functions with a single wave number in the horizontal direction. Such eigenfunctions take the form of left- and right-traveling waves. In many cases the system also has a midplane reflection symmetry. However, when the initial bifurcation is oscillatory, this symmetry is equivalent to evolution in time by half a period and hence has no effect on the dynamics.

The difference in symmetry between the bounded and unbounded systems is crucial, and is present regardless of the aspect ratio of the system. It suggests that while unbounded systems are best described in terms of amplitude equations for the amplitudes of left- and right-traveling waves, bounded systems should be described in terms of odd and even modes (cf. [4]). However, at present, the structure of such modes is unknown [5], except in the simplest of all possible cases, that of Neumann boundary conditions at the sidewalls [6]. These boundary conditions describe stress-free sidewalls with no sideways concentration and heat fluxes. They are special because the resulting eigenfunction can be reflected in the sidewall without introducing a discontinuity in derivatives. As a result, it is possible to generate an eigenfunction of the domain of twice the size by a simple reflection, and thereby embed the problem in a periodic boundary conditions problem with a period twice that of the original domain (cf. [7]). Consequently, the eigenfunctions for Neumann boundary conditions are also harmonic with a single wave number in the horizontal direction. These take the form of uniform amplitude standing waves. However, aside from this special case, one expects eigenfunctions of more complex spatiotemporal behavior, subject only to the requirement of odd or even parity. These are the eigenfunctions that are computed in this paper. These calculations are done for parameter values of experimental interest. Transitions between different modes are studied in detail as a function of the aspect and separation ratios, and their asymptotic properties for large aspect ratios are investigated. Of particular significance is the observation that for large Γ the maximum growth rate and frequency differences between the first two modes that set in both scale as Γ^{-2}. This result supports the description of the system in terms of an interaction between the first odd and even modes [4], and the subsequent interpretation of experimentally observed bursting behavior given in [8].

II. LINEAR STABILITY PROBLEM

We consider a two-dimensional binary fluid mixture in a rectangular container $D\equiv\{x,z|-\frac{1}{2}\Gamma\leqslant x\leqslant\frac{1}{2}\Gamma,-\frac{1}{2}\leqslant z\leqslant\frac{1}{2}\}$ heated uniformly from below. In the Boussinesq approximation appropriate to the experiments, the resulting system is described by the nondimensionalized equations [9]

$$\partial_t \mathbf{u} + (\mathbf{u}\cdot\boldsymbol{\nabla})\mathbf{u} = -\boldsymbol{\nabla} P + \sigma R[\theta(1+S) - S\eta]\hat{\mathbf{z}} + \sigma\nabla^2\mathbf{u}, \tag{2.1a}$$

$$\partial_t \theta + (\mathbf{u}\cdot\boldsymbol{\nabla})\theta = w + \nabla^2\theta, \tag{2.1b}$$

$$\partial_t \eta + (\mathbf{u}\cdot\boldsymbol{\nabla})\eta = \tau\nabla^2\eta + \nabla^2\theta, \tag{2.1c}$$

together with the incompressibility condition

$$\boldsymbol{\nabla}\cdot\mathbf{u} = 0. \tag{2.1d}$$

Here $\mathbf{u}\equiv(u,w)$ is the velocity field in (x,z) coordinates, P, θ, and C denote the departures of the pressure, temperature, and concentration fields from their conduction profiles, and $\eta\equiv\theta - C$. The system is specified by four dimensionless parameters: the separation ratio S, the Prandtl and Lewis numbers σ, τ, and by the Rayleigh number R, in addition to the aspect ratio Γ. The boundary conditions adopted will be those relevant to experiments performed in finite containers. Thus the boundaries will be no-slip everywhere, with the temperature fixed at the top and bottom, and no sideways heat flux. The final set of boundary conditions is provided by the requirement that there is no mass flux through any of the boundaries. The boundary conditions are thus

$$\mathbf{u} = \mathbf{n}\cdot\boldsymbol{\nabla}\eta = 0 \quad \text{on} \quad \partial D \tag{2.2}$$

and

$$\theta = 0 \ \text{ at } \ z = \pm 1/2, \quad \partial_x\theta = 0 \ \text{ at } \ x = \pm\tfrac{1}{2}\Gamma. \tag{2.3}$$

Here ∂D denotes the boundary of D.

To reduce the number of equations involved, we introduce the stream function ψ such that

$$\mathbf{u} = (-\partial_z\psi, \partial_x\psi). \tag{2.4}$$

The nonlinear problem (2.1) can be written in the abstract notation

$$L\phi = N(\phi,\phi), \tag{2.5}$$

where

$$L \equiv \begin{pmatrix} \nabla^2 - \partial_t & \partial_x & 0 \\ \sigma R(1+S)\partial_x & \nabla^2(\sigma\nabla^2 - \partial_t) & -\sigma S\partial_x \\ \nabla^2 & 0 & \tau\nabla^2 - \partial_t \end{pmatrix}, \tag{2.6}$$

N denotes the nonlinear terms, and $\phi\equiv(\theta,\psi,\eta)$. Equation (2.5) is to be solved subject to the boundary conditions

$$\psi = \mathbf{n}\cdot\boldsymbol{\nabla}\psi = \mathbf{n}\cdot\boldsymbol{\nabla}\eta = 0 \quad \text{on} \quad \partial D \tag{2.7}$$

and Eq. (2.3). In this paper we focus our attention on the linear stability properties of the conduction state $\phi\equiv 0$, i.e., the solutions of the linear problem $L\phi = 0$. The nonlinear problem will be the topic of a future paper.

To determine the critical values of the Rayleigh number R at which the conduction state loses stability to overstable convection and the corresponding frequency ω, we look for solutions to the linearized equations of the form

$$\phi = f(x,z)e^{(s+i\omega)t}. \tag{2.8}$$

The condition $s=0$ defines the onset of instability and yields a complex condition that can be solved for R and ω as a function of the aspect ratio Γ for various values of σ, τ, and the separation ratio S. In the following section we summarize our results for two sets of parameters: $\sigma=0.6$, $\tau=0.03$ (typical of ^{3}He/^{4}He mixtures), and $\sigma=18.0$, $\tau=0.012$ (typical of water-ethanol mixtures). These choices are motivated by the experiments of Sullivan and Ahlers [10] and Steinberg *et al.* [2], respectively.

III. RESULTS

In this section we describe the results obtained for two systems, ^{3}He/^{4}He and water-ethanol mixtures, as functions of both the separation ratio of the mixture and the aspect ratio of the container.

A. ^{3}He/^{4}He mixtures

We describe first the results for typical ^{3}He/^{4}He parameters: $\sigma=0.6$, $\tau=0.03$. We begin by describing the results for modest aspect ratios, $4.0\leqslant\Gamma\leqslant 12.0$. Figure 1 shows the eigenvalues $R(\Gamma)$ and $\omega(\Gamma)$ for two values of the separation ratio, $S=-0.001$ and $S=-0.01$, in each case for the first even (solid line) and the first odd (dashed line) mode. For $S=-0.001$, Fig. 1 reveals an oscillatory approach of both sets of curves towards the critical Rayleigh number R_∞ and frequency ω_∞ for an unbounded domain. The braiding of the neutral stability curves $R(\Gamma)$, seen in Fig. 1(a), is familiar from studies of stationary Rayleigh-Bénard convection [11–13], and is found in other systems as well [14]. Because of the braiding, the neutral stability curves for the first odd and first even modes cross repeatedly. Such mode crossings indicate the presence of codimension-two bifurcations. Figure 1(b) shows that at these points the frequencies of the competing modes are distinct. Consequently, these mode interaction points correspond to nonresonant double Hopf bifurcations. However, when $S=-0.01$, the situation changes: for large enough aspect ratios ($\Gamma>10.0$) the two neutral curves develop cusps [Fig. 1(c)]. The presence of these cusps is reflected in the discontinuous jumps in the corresponding frequency curves [Fig. 1(d)]. Figure 2 shows the development of these cusps with decreasing S, focusing on the range $10.0\leqslant\Gamma\leqslant 12.0$. The figure shows the first *two* even (solid lines) and odd (dashed lines) modes at $S=-0.005$ [Figs. 2(a) and 2(b)]; $S=-0.008$ [Figs. 2(c) and 2(d)], and $S=-0.01$ [Figs. 2(e) and 2(f)]. In Fig. 2(a) thick (thin) lines are used to indicate the first (second) mode of each parity and this coding is used to identify the corresponding modes in Figs. 2(c) and 2(e). In the latter the dotted and dashed-dotted curves indicate even and odd modes originating from yet higher modes in Fig. 2(a). Observe that in Fig. 2(a) the neutral stability curves for the two odd modes avoid one another, as do the corresponding curves for the two even modes. At the same time the two sets of frequency curves intertwine. As S decreases the two odd modes come together near $\Gamma=10.5$ and their frequencies coalesce, apparently with the frequency of the primary even mode; similar behavior involving the two even modes takes place near $\Gamma=11.5$ [see Fig. 2(d)]. At somewhat smaller S the two Rayleigh number curves cross transversely [Fig. 2(e)] as the first and second modes of each parity trade places,

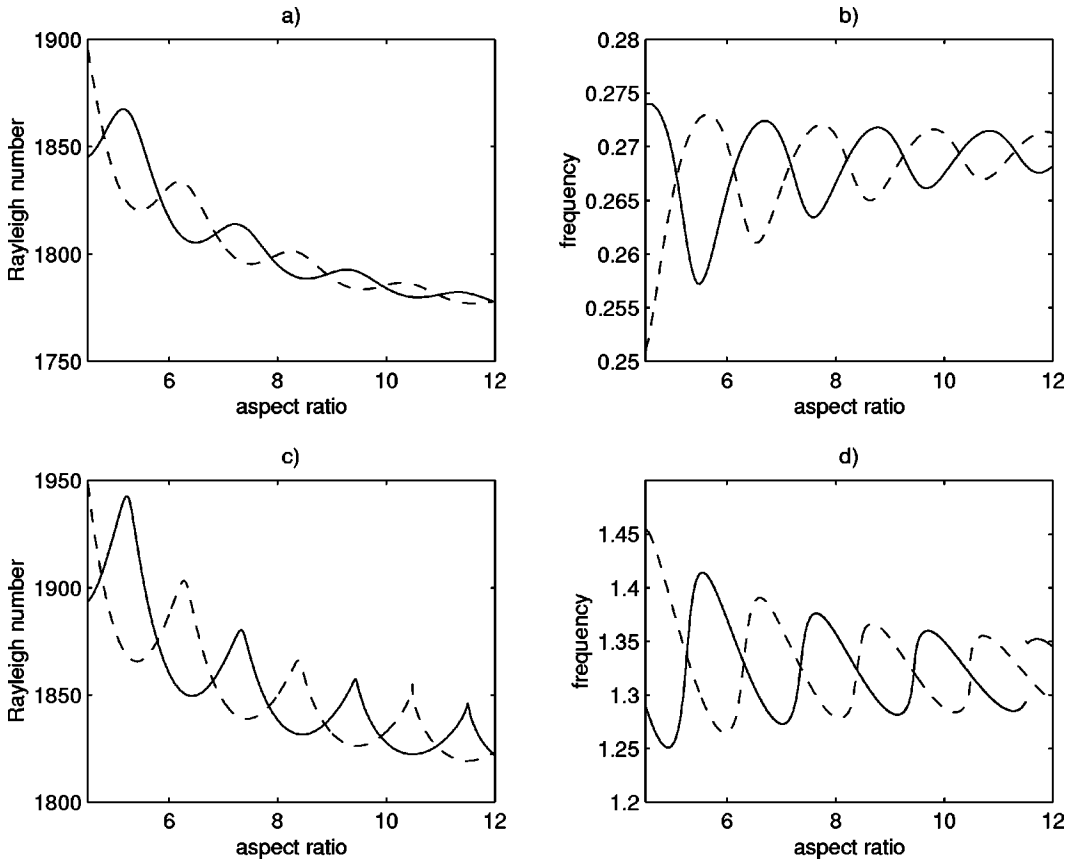

FIG. 1. Onset of convection in ^{3}He/^{4}He mixtures ($\sigma=0.6$, $\tau=0.03$) in moderate aspect ratio containers. (a) Neutral stability curves and (b) corresponding frequencies for the first even (solid line) and odd (dashed line) modes as a function of the aspect ratio Γ for $S=-0.001$. (c) and (d) are the same as (a) and (b) but for $S=-0.01$.

forming the cusps seen in Fig. 1(c). In the range of aspect ratios shown this happens first for the even modes, closely followed by the odd modes. At the same time the corresponding frequency curves separate and thereafter no longer cross. The same interchange mechanism is also responsible for the appearance of the cusp in the second even mode neutral stability curve near $\Gamma=10.3$ with a yet higher order even mode involved (dotted line), with similar behavior occurring for the second odd mode near $\Gamma=11.3$ as well [Fig. 2(c)].

This type of behavior can be understood as follows. Consider first the case of stationary convection in a finite box. In this case the neutral stability curves for the first odd and even modes are braided much as in Fig. 1(a), and so are the corresponding curves for the second odd and even modes, etc. These families do not interact, i.e., the primary instability is always to either an odd or an even mode from the first family. In this case it is known that as $\Gamma\to\infty$ the gap between adjacent families is $\mathcal{O}(\Gamma^{-2})$, while the amplitude of the oscillations in the neutral curves is only $\mathcal{O}(\Gamma^{-3})$, i.e., when the aspect ratio is large enough a gap opens up between the first family of neutral curves and the next [11,13,15]. In the case of oscillatory onset the situation is more complex. For fixed S, however small, the braiding behavior continues for moderate aspect ratios, but with increasing Γ the different families of neutral curves begin to interact and the even and odd modes that come in first can be traced to successively higher families. The necessary crossing between modes of like parity originating in adjacent families is mediated by 1:1 resonances located at discrete points $(R_c^{(3)},\Gamma_c^{(3)},S_c^{(3)})$ in the three-dimensional parameter space (R,Γ,S) as we now describe.

At each 1:1 resonance the linear problem takes the form

$$\begin{pmatrix}\dot z_1\\ \dot z_2\end{pmatrix}=\begin{pmatrix}i\omega_c^{(3)} & 1\\ 0 & i\omega_c^{(3)}\end{pmatrix}\begin{pmatrix}z_1\\ z_2\end{pmatrix}, \tag{3.1}$$

where z_1 and z_2 are the complex amplitudes of the first two like-parity modes. Here $\omega_c^{(3)}$ is the resonant frequency. This Jordan block form arises because both modes have the *same* symmetry. In contrast, a 1:1 resonance between an odd and an even mode would have a diagonal linearization; the intersection of the corresponding neutral curves is then robust under perturbations (unfolding) of the normal form. This is not so when both modes have like parity. Since the 1:1 resonance is a codimension-three phenomenon [it is necessary to choose $R_c^{(3)}$, $\Gamma_c^{(3)}$ to locate the crossing of the neutral stability curves, and vary a third parameter (here S) to match the frequencies at the crossing point], the most general deformation of the Jordan block appearing in Eq. (3.1) depends on three real parameters. The resulting linear system is [16]

$$\begin{pmatrix}\dot z_1\\ \dot z_2\end{pmatrix}=\begin{pmatrix}i\omega_c^{(3)}+\alpha & 1\\ \mu_1+i\mu_2 & i\omega_c^{(3)}+\alpha\end{pmatrix}\begin{pmatrix}z_1\\ z_2\end{pmatrix} \tag{3.2}$$

and leads to the characteristic equation

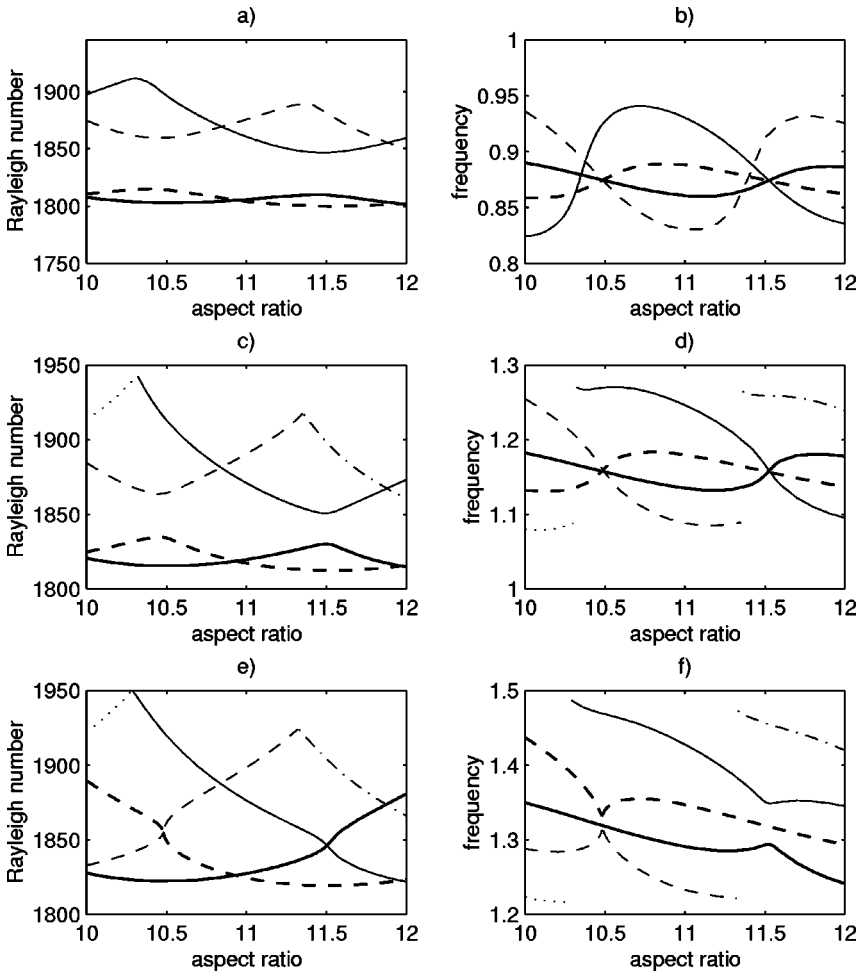

FIG. 2. Details of the reconnection process between two modes of like parity for (a) and (b) $S=-0.005$, (c) and (d) $S=-0.008$, and (e) and (f) $S=-0.01$, when $\sigma=0.6$, $\tau=0.03$. In (a) solid (dashed) lines denote even (odd) modes, while thick (thin) lines denote first (second) modes of each type.

$$(s-\alpha-i\omega_c^{(3)})^2-\mu_1-i\mu_2=0 \tag{3.3}$$

for solutions of the form $\exp st$. To find the neutral curves we set $s=i\omega$ and obtain the two real equations

$$(\omega-\omega_c^{(3)})^2+\mu_1-\alpha^2=0, \quad 2\alpha(\omega-\omega_c^{(3)})+\mu_2=0. \tag{3.4}$$

It follows that

$$\alpha^2=\frac{1}{2}(\mu_1+\sqrt{\mu_1^2+\mu_2^2}) \tag{3.5}$$

and

$$(\omega-\omega_c^{(3)})^2=\frac{1}{2}(-\mu_1+\sqrt{\mu_1^2+\mu_2^2}). \tag{3.6}$$

We now examine these relations in turn. It is convenient to think of Eq. (3.5) as describing the dependence of α on μ_2 for fixed μ_1. When $\mu_1>0$, $|\alpha(\mu_2)|\geqslant\sqrt{\mu_1}$ with zero slope at $\mu_2=0$, and $\alpha\approx\pm\sqrt{|\mu_2|}/2$ for $|\mu_2|\gg\mu_1$. Consequently, when μ_1 is small, the curve $|\alpha(\mu_2)|$ has a narrow but rounded minimum at $\mu_2=0$, but rapidly becomes convex as $|\mu_2|$ increases away from zero. A tendency towards this type of behavior can be seen in Fig. 2(c) near $\Gamma=11.5$ and becomes more and more pronounced as the two even mode neutral curves approach one another. Moreover, when $\mu_1<0$ and $|\mu_2|\ll|\mu_1|$, one finds that locally $\alpha(\mu_2)$ takes the form of a pair of straight lines through the origin, $\alpha=\pm\frac{1}{2}|\mu_1|^{-1/2}\mu_2$, with the same $\pm\sqrt{|\mu_2|/2}$ behavior for $|\mu_2|\gg|\mu_1|$. Thus when $|\mu_1|$ is small the slope of the lines through the origin is large. This type of behavior can be seen near the crossing of the two odd modes in Fig. 2(e) ($\Gamma\approx10.5$). Together these observations suggest that we identify α, μ_1, and μ_2 with $\Delta_R\equiv(R-R_c^{(3)})/R_c^{(3)}$, $\Delta_S\equiv(S-S_c^{(3)})/S_c^{(3)}$, and $\Delta_\Gamma\equiv(\Gamma-\Gamma_c^{(3)})/\Gamma_c^{(3)}$, respectively, in place of the more general linear relation

$$(\mu_1,\mu_2,\alpha)^T=M(\Delta_S,\Delta_\Gamma,\Delta_R)^T+\cdots, \tag{3.7}$$

where M is a constant 3×3 matrix. We return to this point below.

This identification is supported by the behavior of the frequency ω as a function of μ_2. When $\mu_1>0$, Eq. (3.6) shows that $\omega-\omega_c^{(3)}$ takes the form of two straight lines crossing at the origin, and convex away from $\mu_2=0$. The slope of these lines at the origin, $\pm\frac{1}{2}\mu_1^{-1/2}$, is large when μ_1 is small, with the result that the two positive branches of $\omega-\omega_c^{(3)}$ form a cusp at the origin, as do the two negative branches, i.e., the curves cross [see Fig. 2(d)]. When $\mu_1<0$, $|\omega-\omega_c^{(3)}|=\sqrt{-\mu_1}$ at $\mu_2=0$ with zero slope there and convex behavior for $|\mu_2|\gg|\mu_1|$. In other words, the cusp lifts off the axis and becomes differentiable as the two frequency curves cease crossing and detach [Fig. 2(f)]. This process is the reverse of what happens in the $\alpha(\mu_2)$ curves, and accounts for the (local) resemblence between the Ray-

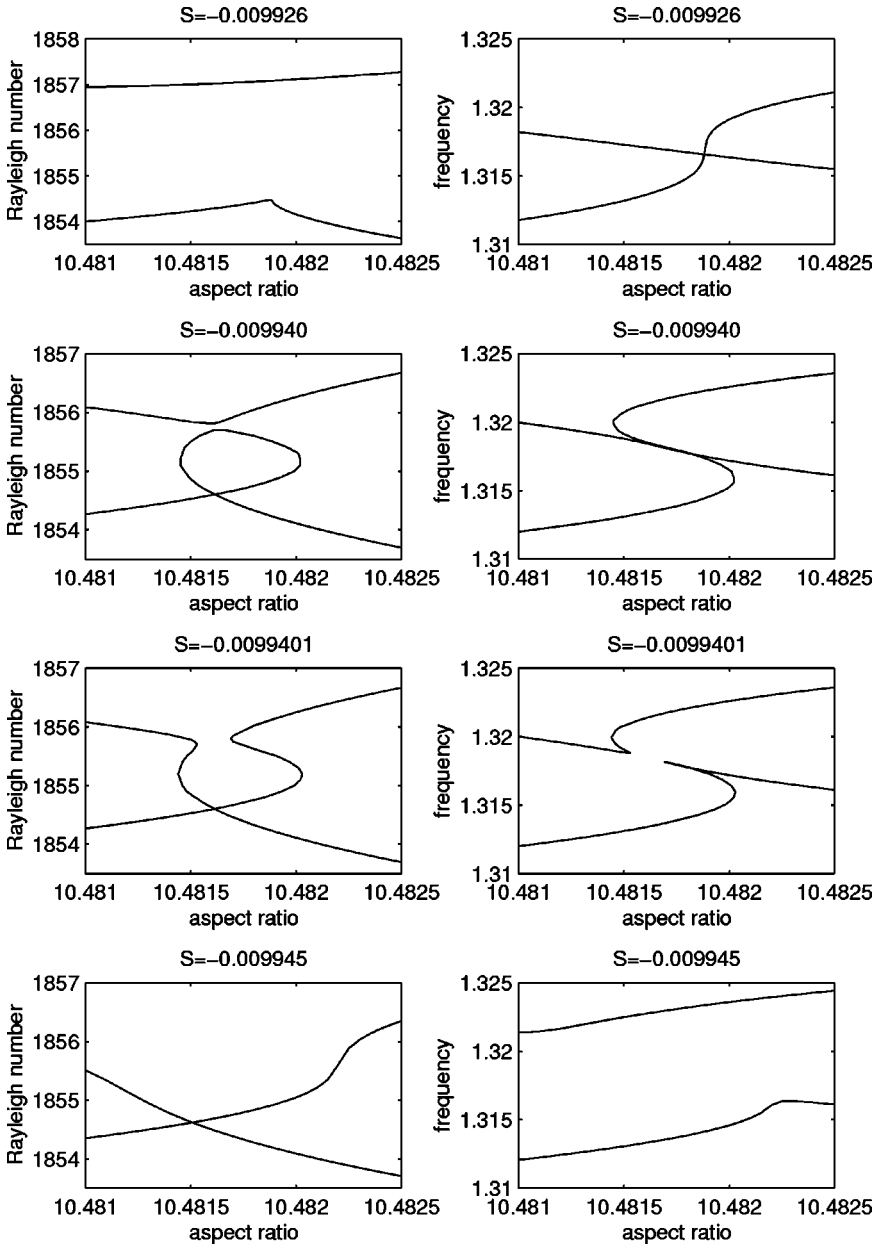

FIG. 3. Details of the passage through 1:1 resonance at $R_c^{(3)} = 1855.80$, $\Gamma_c^{(3)} = 10.4816$, $S_c^{(3)} = -0.00994$, showing the formation of a small loop prior to the resonance.

leigh number plot for $S > S_c^{(3)}$ and the frequency plot for $S < S_c^{(3)}$, and vice versa. The origin of the frequency jump seen in Fig. 1(d) for $S = -0.01$ is now clear: if one follows the neutral stability curve for the *first* even mode to set in [Fig. 2(e)], one must switch at the mode crossing point from the thick solid frequency curve to the thin one. Such frequency jumps are thus the result of the detachment of the frequency curves at the 1:1 resonance. Note that away from $S = S_c^{(3)}$ the two odd and the two even neutral curves cross in a structurally stable way. This is because the frequencies at the mode crossings are now nonresonant [cf. Fig. 2(f)].

Note also that the critical frequency $\omega_c^{(3)}$ of the two odd modes appears to coincide with the frequency of one of the even modes, and vice versa. Despite this coincidence (which we do not understand), this even mode is not in resonance with the two odd modes; it sets in at a lower value of R and is therefore already unstable. Consequently, all of the complex dynamics associated with the odd-odd 1:1 resonance [16] are unstable to even parity perturbations and vice versa, i.e., the 1:1 resonances are always *shielded*. Nonetheless, as indicated above, these resonances provide the key to modal exchange between like-parity modes as the aspect ratio of the system is increased and hence to the fact that different modes ultimately set in as primary modes as Γ increases. Loosely speaking, these modes differ in the number of ''rolls'' present, although in the present system this number is not constant along any continuous neutral curve. This is a consequence of the non-Neumann boundary conditions at the sidewalls (cf. [13]).

The above theory apparently provides a complete description of the transformation of the neutral stability curves at the 1:1 resonance. In fact, a careful examination of the resonance near $\Gamma = 10.5$ reveals an unexpected surprise. Figure 3 summarizes what happens: as the resonance is approached, the first odd mode develops a cusp before the mode ''crossing'' takes place. This cusp is associated with a hysteresis ''bifurcation'' in its frequency. As $|S|$ increases the cusp turns into a loop that grows in size as the two neutral stabil-

ity curves approach one another. At the 1:1 resonance the two neutral curves touch, and so do the corresponding frequency curves. However, in contrast to the theory described above, both do so with an orientation that is opposite of that predicted. With further increase in $|S|$ both sets of curves reconnect and move apart, eventually producing the mode crossing shown in Figs. 2(e) and 2(f). Thus at the actual 1:1 resonance no mode crossing in fact takes place; the mode crossing seen in Fig. 2(e) is in fact formed when the neutral stability curve first develops the loop. This type of mode interaction can also be described by the above theory, but requires a conversion from the unfolding parameters to those used in the calculations. This conversion is nonlinear. If we suppose that $(\Delta_S,\Delta_\Gamma,\Delta_R)=\mathcal{O}(\epsilon)$, $\epsilon\ll 1$, and examine the relations (3.4) we are forced to conclude that at leading order $\mu_{1,2}=\mathcal{O}(\epsilon^2)$, while α and $\omega-\omega_c^{(3)}$ are both $\mathcal{O}(\epsilon)$. Thus $\mu_{1,2}$ are in fact both *quadratic* functions of $\Delta_S,\Delta_\Gamma,\Delta_R$, in contrast to the naive relation (3.7). It follows that the relation between $\mu_{1,2}$ and α given by Eqs. (3.4) is *quartic* in $\Delta_S,\Delta_\Gamma,\Delta_R$. When $\Delta_S=0$ the resulting relation between Δ_R and Δ_Γ has either two or four real roots, describing the two types of mode crossings that can occur in these variables, but the detailed appearance depends on the coefficients. It is likely that a similar nonlinear relation between the unfolding and physical parameters is also responsible for the formation of the cusp seen in Fig. 3 even though the normal form (3.2) is not an unfolding of this degeneracy.

We have used Fig. 3 and similar figures to locate three 1:1 resonances:

$$R_c^{(3)}=1855.80,\ \ \Gamma_c^{(3)}=10.4816,\ \ S_c^{(3)}=-0.00994, \tag{3.8a}$$

$$R_c^{(3)}=1803.80,\ \ \Gamma_c^{(3)}=19.8062,\ \ S_c^{(3)}=-0.006028, \tag{3.8b}$$

$$R_c^{(3)}=1784.15,\ \ \Gamma_c^{(3)}=34.2444,\ \ S_c^{(3)}=-0.00403. \tag{3.8c}$$

The resonant frequencies at these points are 1.318, 0.976, and 0.76, respectively. The first of these resonances is shown in Fig. 3; the next is also associated with loop formation, although the loop is much smaller. Specifically, if we characterize the loop in the $\Gamma\approx 10$ container by its size, $\Delta R\approx 1.5$, and extent, $\Delta S\approx 10^{-5}$, in the $\Gamma\approx 20$ container the corresponding quantities are $\Delta R\approx 0.5$ and $\Delta S\approx 10^{-6}$. For the third resonance, near $\Gamma=34$, the loop (if it exists) is too small to be resolved. Thus the loops apparently disappear as Γ increases.

In contrast to the codimension-three bifurcations just discussed the codimension-two odd/even interactions are not shielded. Consequently, the dynamics arising from the interaction between the first odd and even modes is observable in the nonlinear problem. At these bifurcations the linear problem takes the form

$$\begin{pmatrix}\dot z_+\\ \dot z_-\end{pmatrix}=\begin{pmatrix} i\omega_{c+}^{(2)} & 0\\ 0 & i\omega_{c-}^{(2)}\end{pmatrix}\begin{pmatrix} z_+\\ z_-\end{pmatrix}, \tag{3.9}$$

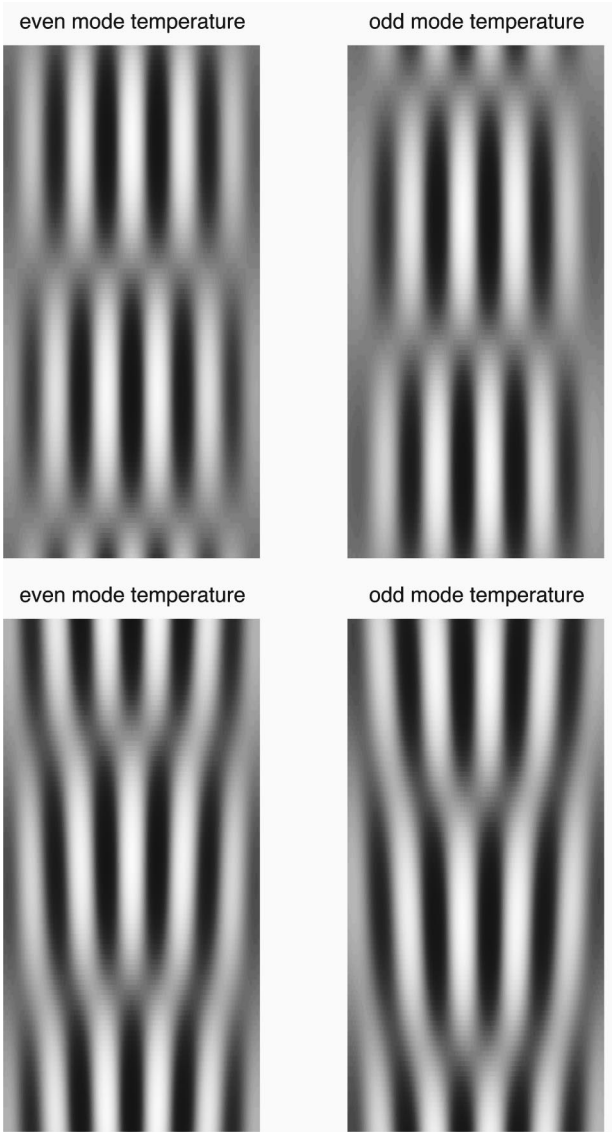

FIG. 4. Space-time diagrams, with time increasing upwards, showing the evolution of the midplane temperature as a function of location x in a $\Gamma=10.0$ container, $-5.0\leqslant x\leqslant 5.0$. Top panels, $S=-0.001$; bottom panels, $S=-0.01$. The eigenfunctions in the former case are standing waves, but become chevronlike states in the latter.

where $z_\pm$ denote the complex amplitudes of the even $(+)$ and odd $(-)$ modes, respectively. The unfolded linear problem is then given by

$$\begin{pmatrix}\dot z_+\\ \dot z_-\end{pmatrix}=\begin{pmatrix} \mu_+ + i\omega_+ & 0\\ 0 & \mu_- + i\omega_-\end{pmatrix}\begin{pmatrix} z_+\\ z_-\end{pmatrix}, \tag{3.10}$$

where $\mu_\pm$ represent the growth rates of the two modes and $\omega_\pm-\omega_{c\pm}^{(2)}=\mathcal{O}(\mu_\pm)$. These growth rates vanish at the mode crossings, hereafter denoted by $(R_c^{(2)},\Gamma_c^{(2)})$. As already mentioned these results remain valid even if $\omega_{c+}^{(2)}=\omega_{c-}^{(2)}$, i.e, even at resonance.

In Fig. 4 we show the first even and odd temperature modes for $\Gamma=10.0$ when $S=-0.001$ (top panels) and $S=-0.01$ (lower panels). The modes are shown in the form of space-time diagrams, with time increasing upwards. When

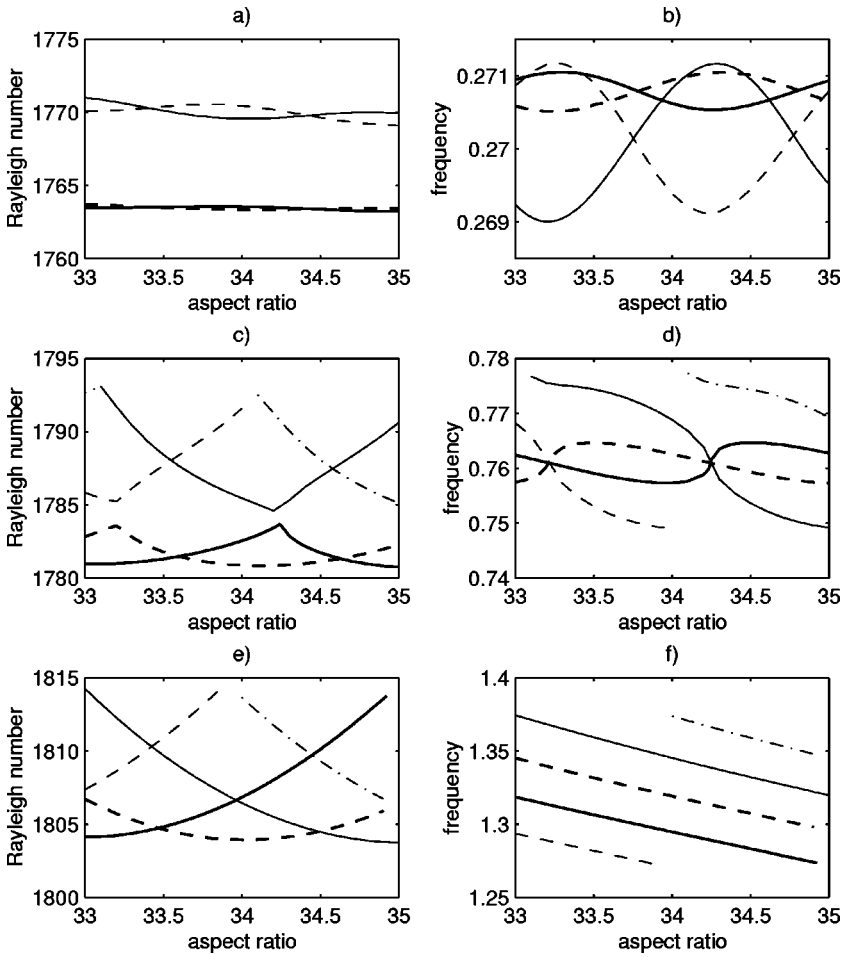

FIG. 5. Neutral stability curves and onset frequencies for convection in ^{3}He/^{4}He mixtures ($\sigma = 0.6$, $\tau = 0.03$) in large aspect ratio containers when (a) and (b) $S = -0.001$, (c) and (d) $S = -0.004$, and (e) and (f) $S = -0.01$. In (a) solid (dashed) lines denote even (odd) modes, while thick (thin) lines denote first (second) modes of each type.

$S = -0.001$ both eigenfunctions take the form of standing waves, with the dynamics either in phase at the two sidewalls (even mode) or out of phase (odd mode). The amplitude of the standing oscillations peaks in the middle of the containers and decreases towards the sidewalls. There is a considerable phase lag (not shown) between the temperature and concentration oscillation, a consequence of the small value of τ. In both cases the wavelength of the standing waves is almost uniform across the cell, in contrast to the amplitude.

As S decreases the eigenfunctions gradually develop into ''chevronlike'' states, as indicated in the space-time diagrams for $S = -0.01$. Both even and odd modes consist of waves propagating outward from the container center and modulated in amplitude at the Hopf frequency ω. In particular, away from the center of the container the node lines are now defined for all time and these propagate slowly when the amplitude is large and rather more rapidly when it is small. Thus the resulting oscillation has the form of a large-amplitude near-stationary state followed by a shorter smaller-amplitude propagative phase during which the node translates outwards by half a wavelength, followed by another large-amplitude near-stationary phase, etc. Despite its complexity the resulting oscillation is of course sinusoidal in time. Also of interest is the fact that nodes are continually born in the middle of the container. This is necessary if waves continually propagate outwards, but it indicates that quite complex behavior with sources (or sinks) is readily described by *linear* eigenfunctions, i.e., there is nothing intrinsically nonlinear about such features. Note, however, that the amplitude of the eigenfunctions still peaks in the center and that the wavelength of both modes remains essentially constant across the container.

It is of interest to compare the above results with those for $\Gamma = 34.0$, the aspect ratio used by Sullivan and Ahlers [10]. In Fig. 5 we show the neutral stability curves and corresponding frequencies for the first four modes in the range $33.0 \leqslant \Gamma \leqslant 35.0$ for $S = -0.001$, $S = -0.004$, and $S = -0.01$. A comparison with Figs. 1 and 2 reveals that the frequencies of the dominant modes are evidently determined primarily by the fluid parameters and not the aspect ratio. This is because the oscillations are bulk oscillations that are modified but not caused by the presence of sidewalls. Figure 5(a) shows that when $|S|$ is sufficiently small the first two families of neutral curves are separated by a gap that is much larger than the amplitude of the braids within each family. This is typical of what happens in Rayleigh-Bénard convection with non-Neumann boundary conditions [13]. However, in the case of overstability this behavior changes as $|S|$ increases [Fig. 5(c)] and begins to look like that shown in Fig. 5(e). This figure shows the neutral curves for $S = -0.01$ but the same range of Γ, and reveals the crossing of adjacent even modes. This mode crossing involves a *nonresonant* double Hopf bifurcation [Fig. 5(f)] and is the result of a resonant 1:1 mode crossing at $S = -0.00403$ [see Figs. 5(c) and 5(d)], i.e., it is formed by the same process as that leading to the nonresonant crossings shown in Figs. 2(e) and 2(f). The fact that the frequency curves in Fig. 5(f) are essentially parallel ''straight lines'' confirms that this mode crossing is

''far'' from the 1:1 resonance at $S=-0.00403$. The figure is also in agreement with the plausible hypothesis that in large aspect ratio systems the frequencies of the first few modes must take the form

$$\omega_n \sim \omega_\infty + c_{1n}\Gamma^{-1} + c_{2n}\Gamma^{-2} + \cdots, \quad n=1,2,\ldots, \tag{3.11}$$

where the index n specifies the order in which the modes become primary as Γ increases. Thus the nth mode is primary in the interval $\Gamma_{n-1} \leqslant \Gamma \leqslant \Gamma_n$, etc. It follows that $n = \mathcal{O}(\Gamma)$. The results of Fig. 5 suggest that $c_{1n} \sim c_1$, $c_{2n} \sim n c_2$, where c_1 and c_2 are $\mathcal{O}(1)$ constants independent of n and Γ. Then, at any (large) Γ, there is an $\mathcal{O}(\Gamma^{-1})$ correction to ω_∞, while $\triangle_n\omega \equiv \omega_{n+1} - \omega_n = \mathcal{O}(\Gamma^{-2})$. Thus near any particular Γ the quantity $\triangle_n\omega$ takes the form, as a function of Γ, of a set of equally spaced, almost horizontal, lines. We have checked that similar behavior occurs for $S=-0.021$ as well. Figure 5 therefore suggests that for large Γ the splitting $\triangle\omega$ in frequency and $\triangle R$ in Rayleigh number between the first odd and even modes are both of the *same* order as $\Gamma \to \infty$. As discussed in Sec. IV, this conclusion implies that the normal form describing the interaction between odd and even modes in the large aspect ratio limit has approximate D_4 symmetry, as argued by Landsberg and Knobloch [4].

Figure 6 shows the first odd temperature eigenfunction for $S=-0.001$ and $S=-0.021$, again in the form of space-time diagrams. In the former case the eigenfunction now consists of a pair of waves traveling *inwards*, with the center of the container serving as a sink. Once again the wavelength is very uniform across the container despite the fact that the amplitude varies substantially (lower left panel). When $S=-0.021$ the direction of propagation is outwards with the center of the container having become a source. The amplitude now has a local minimum at the center and increases outwards, peaking near the sidewalls (lower right panel). This type of eigenfunction was anticipated by Cross [17], and is characteristic of eigenfunctions in systems with *positive* group velocity. In our finite system we cannot, strictly speaking, define a group velocity since the allowed wave number is quantized by the sidewalls, as well as being nonuniform. However, for the purposes of the present paper the most important observation is that for aspect ratios this large the odd and even eigenfunctions are essentially indistinguishable, as hypothesized by Landsberg and Knobloch [4].

As is well known, oscillations in binary mixtures are present only for sufficiently large $|S|$. We have examined the effect of sidewalls on the transition from oscillatory onset to steady onset as $|S|$ decreases. For $\Gamma \approx 10$ these results are summarized in Fig. 7. As $|S|$ is decreased for $\Gamma=9.7$ the frequency (not shown) of the first mode (an odd mode) decreases smoothly to zero at $S \equiv S_{TB} \approx -0.000516$ and, thereafter, a steady mode of the same parity is preferred. The zero frequency point is known as a Takens-Bogdanov point; at such a point the linearization takes the form

$$\begin{pmatrix} \dot{p} \\ \dot{q} \end{pmatrix} = \begin{pmatrix} 0 & 1 \\ 0 & 0 \end{pmatrix} \begin{pmatrix} p \\ q \end{pmatrix}, \tag{3.12}$$

where $p(t)$ is a real amplitude and

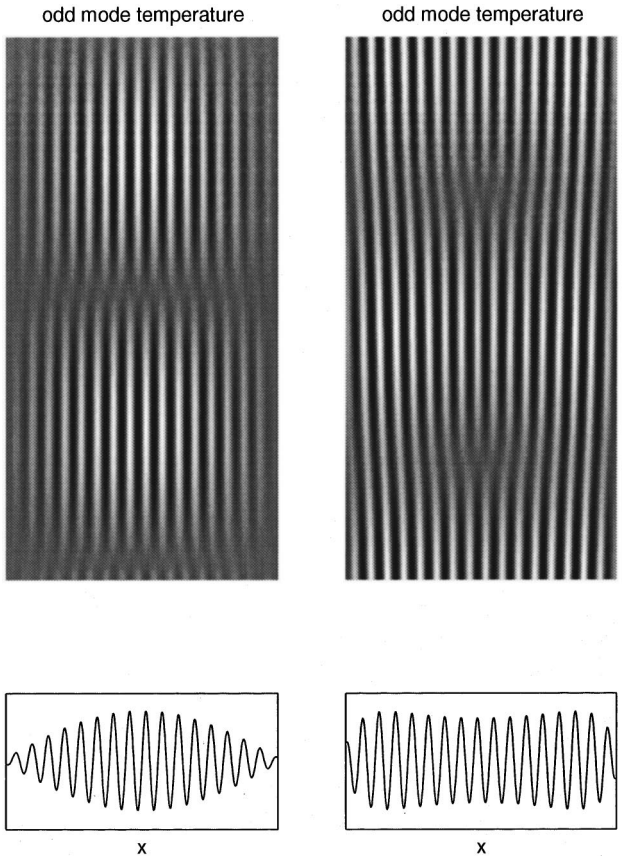

FIG. 6. Space-time plots of the midplane temperature, with time increasing upwards, showing the evolution of the first unstable mode as a function of location x in a $\Gamma=34.0$ container, $-17.0 \leqslant x \leqslant 17.0$. Top left panel, $S=-0.001$; top right panel, $S=-0.021$. The lower panels show the corresponding midplane temperature profiles at $t=0.3T$, $t=0.5T$, respectively, where T is the Hopf period.

$$\theta(x,z,t) = p(t) f_-(x,z) + \cdots. \tag{3.13}$$

The Takens-Bogdanov point is of codimension two and its unfolding is given by

$$\begin{pmatrix} \dot{p} \\ \dot{q} \end{pmatrix} = \begin{pmatrix} 0 & 1 \\ \mu & \nu \end{pmatrix} \begin{pmatrix} p \\ q \end{pmatrix}, \tag{3.14}$$

where μ and ν are real unfolding parameters related to $R - R_{TB}$ and $S - S_{TB}$. For $\Gamma=9.8$ the situation changes. As $|S|$ decreases an oscillatory odd mode is now superseded by a steady even mode at $S \approx -0.000532$, while the oscillatory mode still has a finite frequency. The resulting transition is a Hopf steady state interaction, and is also of codimension two. A similar transition occurs when $\Gamma=9.9$. Finally, when $\Gamma=10.0$ the even mode is preferred on either side of the Takens-Bogdanov transition and remains so until $\Gamma=10.7$ where an odd mode begins to take over again. The transition at $\Gamma=34.0$ is also an interaction between an oscillatory odd mode and a steady even mode, and occurs at $S=-0.000555$ and $R=1761.55$. It is of interest to compare these results with those for an unbounded layer with periodic boundary conditions [18]. Here the Takens-Bogdanov point is *always* shielded by an oscillatory instability that precedes

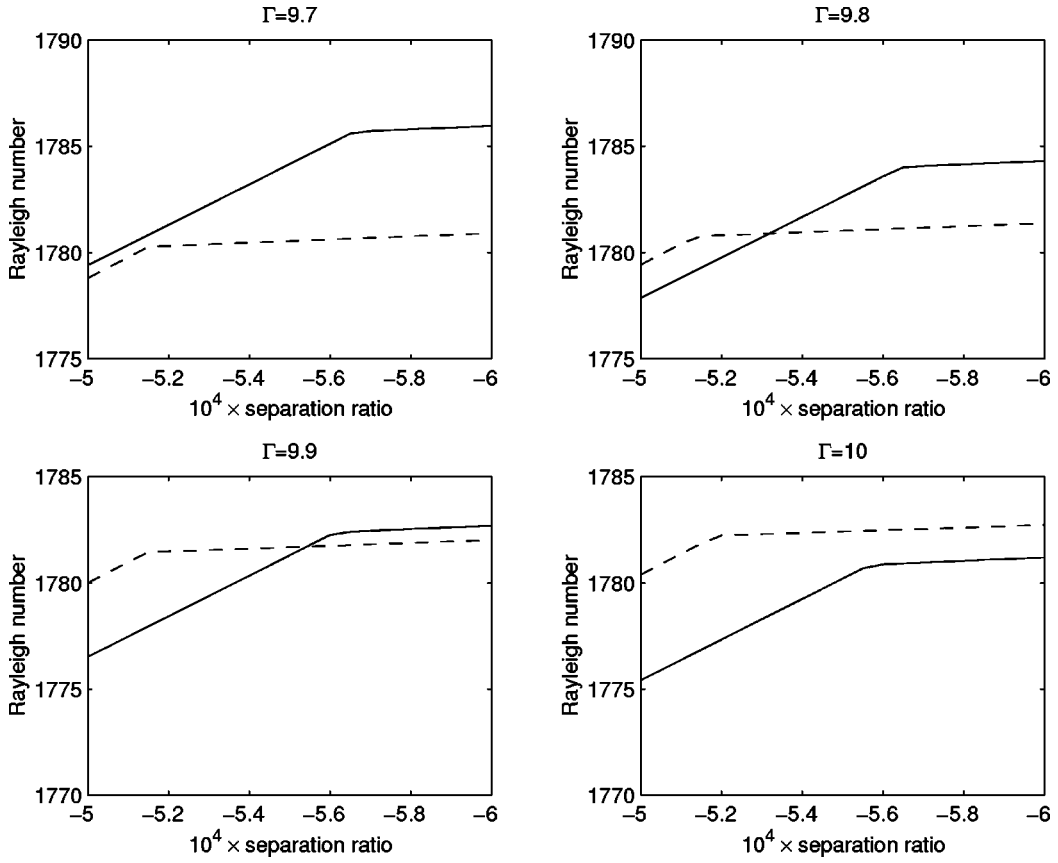

FIG. 7. Transition between oscillatory and steady onsets as a function of the separation ratio for the first even (solid lines) and first odd (dashed lines) modes for aspect ratios near $\Gamma=10$ and $\sigma=0.6$, $\tau=0.03$. (a) $\Gamma=9.7$, (b) $\Gamma=9.8$, (c) $\Gamma=9.9$, and (d) $\Gamma=10.0$. The lines to the left (right) of the break in slope correspond to steady (oscillatory) onset.

it. Specifically, $R_{TB}\approx 1758.2$ and $S_{TB}\approx -0.000530$ with wave number $k_{TB}=3.0754$, but the transition to steady convection takes place already at $S\approx -0.000544$. At this S steady convection sets in at $R=1758.18$ and has the wave number $k=3.1420$. However, in contrast to the finite container situation this transition cannot be described by a finite-dimensional Hopf steady state normal form because the wave numbers at this transition are effectively incommensurate. Although the shielding effect is evidently small it does imply that in an unbounded system the dynamics associated with the Takens-Bogdanov point may be unobservable. In contrast, in a finite system, our calculations indicate that the shielding of the Takens-Bogdanov point is relatively rare (it occurs for about 18% of the aspect ratios near $\Gamma=10$) and indeed dynamics associated with such a point have been detected in experiments [19]. The Hopf steady state interactions are also, in principle, observable. Note that by varying the aspect ratio it should be possible to locate several codimension-3 bifurations. A double Takens-Bogdanov bifurcation at which the first odd and even modes both have zero frequency simultaneously may be accessible. As of now this codimension-three bifurcation has not been studied and specific predictions about the resulting dynamics cannot be made.

B. Water-ethanol mixtures

In Fig. 8 we show the critical Rayleigh numbers and associated frequencies for the first even and odd mode for water-ethanol mixtures ($\sigma=18.0$, $\tau=0.012$) for $4.0\leqslant\Gamma\leqslant 12.0$ and $S=-0.001$ [Figs. 8(a) and 8(b)] $S=-0.01$ [Figs. 8(c) and 8(d)]. Except for quantitative differences, the behavior of these curves resembles strongly that shown in Fig. 1 for He^3/He^4 mixtures. In particular, we see again the formation of cusps with increasing aspect ratio, indicating the presence of mode crossing. The resulting eigenfunctions are qualitatively similar as well. Indeed, a stable chevronlike pattern has been observed near onset in an ethanol-water mixture with these parameter values ($\tau=0.012$, $\sigma=18$) at $S=-0.014$ [2]. Weakly nonlinear calculations in an unbounded domain with these parameter values show that stable chevrons are first present when S exceeds -0.011 [9], in close correspondence with the experimental observation. The fact that these states occur stably in such a limited range of S may explain why they have been observed in so few experiments.

IV. DISCUSSION

In this paper we have described in detail the onset of oscillatory convection in a two-dimensional container with realistic boundary conditions applied on all four boundaries. These results indicate that the sidewalls introduce a number of complications into the system even if the aspect ratio is quite large. We have seen that the competition between odd and even modes in such a system takes one of two basic forms, depending on the separation and aspect ratios (see Fig. 9). When $|S|$ is small (i.e., close to S_{TB}) and Γ is not too large, the mode interaction takes the form familiar from

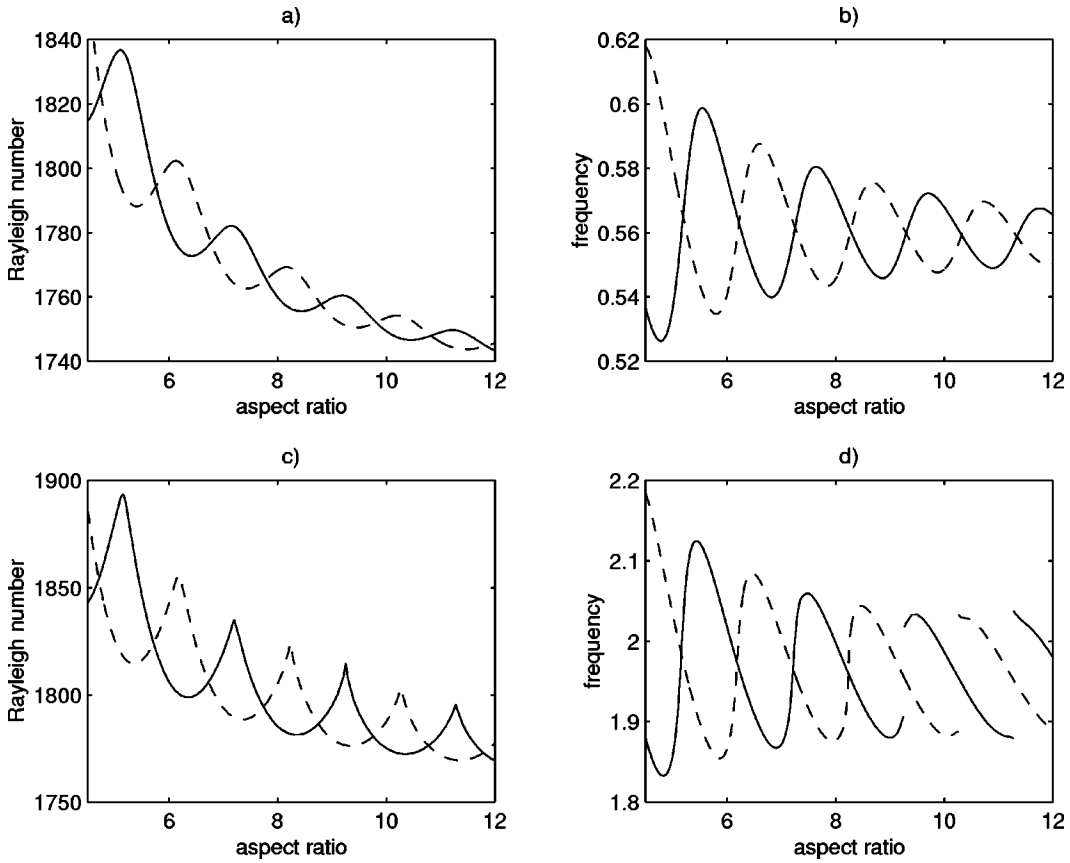

FIG. 8. Onset of convection in water-ethanol mixtures ($\sigma=18$, $\tau=0.012$) in moderate aspect ratio containers. (a) Neutral stability curves and (b) corresponding frequencies for the first even (solid line) and odd (dashed line) modes as a function of the aspect ratio Γ for $S=-0.001$. (c) and (d) are the same as (a) and (b) but for $S=-0.01$.

Rayleigh-Bénard convection with non-Neumann boundary conditions: the neutral curves $R(\Gamma)$ divide neatly between different families and there is no intermingling among them [see Fig. 5(a)]. Each family consists of a pair of braided neutral curves, one for an odd mode and the other for an even mode, with each family well separated from the next, at least for the low-lying families. The crossings between odd and even modes within each family are structurally stable because of their different parity. At fixed Γ and large enough $|S|$ the situation is quite different [see Fig. 5(c)]. There are now no distinct families of neutral curves and all modes (including like-parity modes) cross. These mode crossings are all structurally stable, either because the modes have opposite parity, or because their frequencies at the mode crossings are nonresonant. The transition between these two types of behavior occurs via 1:1 resonant mode interactions as illustrated in Fig. 2. These interactions allow mode crossings between like-parity modes belonging to different families and hence are responsible for the transition between the neutral stability curves in Figs. 5(a) and 5(c). Likewise, at fixed S the neutral stability curves are braided when the aspect ratio Γ is not too large, but with increasing Γ nonresonant crossings between like-parity modes appear (cf. Fig. 2), as anticipated by Hirschberg and Knobloch [13]. We have also seen that in a finite system the Takens-Bogdanov point is likely to be accessible to experimental study if the aspect ratio is chosen appropriately, and likewise for Hopf steady state interactions between opposite parity modes. Both observations may shed light on the experiments [10,20]. On the basis of our calculations we have made several conjectures about the behavior of the neutral stability curves and corresponding frequencies and eigenfunctions for large aspect ratios. These bear out the picture of large aspect ratio systems put forward by Landsberg and Knobloch [4] with two significant clarifications. First, we have found that if the separation ratio is small there is a substantial range of aspect ratios within which the first odd and even modes to set in are separated from the next pair by a significant gap in Rayleigh number. In this range the existence of the gap justifies the reduction of the partial differential equations to amplitude equations for the first odd and even modes only. We have presented examples of what these modes look like. However, for sufficiently large aspect ratios or sufficiently large separation ratios this gap disappears, and odd and even modes from different families are selected in succession. In this case the reduction to a pair of amplitude equations continues to be valid near all crossing points between odd and even modes, but it is no longer clear whether such a description captures the behavior of the system for all intervening aspect ratios. Second, we have found that the frequency difference between the competing odd and even parity modes scales as Γ^{-2} for large Γ instead of the expected Γ^{-1} behavior. This observation strengthens the argument in favor of Ref. [4] as we now describe.

In Ref. [4] Landsberg and Knobloch suggested that weakly nonlinear overstable systems in large aspect ratio containers are properly described by the normal form equations for a double Hopf bifurcation with broken D_4 symme-

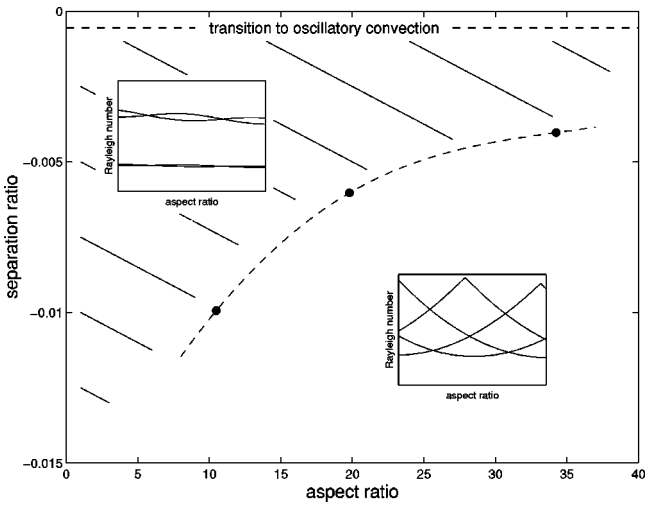

FIG. 9. The (Γ,S) plane showing the approximate location of mode avoidance (hatched region) and mode crossing (unhatched region).

try, and used this approach to suggest an explanation for the intermittent bursting observed at the onset of convection by Sullivan and Ahlers [10]. The details of the bursting mechanism are described in Ref. [8]. The mechanism relies on the presence of approximate D_4 symmetry for the formation of global connections to ''infinity'' and back again; excursions along these connections are identified with the observed bursts. The D_4 symmetry arises naturally in these systems. Recall that the amplitude equations describing the interaction of the first odd and even modes must be equivariant with respect to

$$(z_+,z_-)\to(z_+,-z_-), \tag{4.1}$$

owing to the reflection symmetry $x\to -x$, $(\theta,\psi,\eta)\to(\theta,-\psi,\eta)$ of the original system [Eqs. (2.5)–(2.7)]. Landsberg and Knobloch argued that in the large aspect ratio limit there is, in addition, an interchange symmetry between the odd and even modes since these are effectively indistinguishable throughout most of the domain. Thus the normal form should also be equivariant under

$$(z_+,z_-)\to(z_-,z_+). \tag{4.2}$$

These two reflections generate the symmetry D_4. However, since the interchange symmetry is not exact for any finite Γ (at any finite Γ the first mode is either odd or even, except for a discrete set of Γ) this D_4 symmetry is broken. Since the dominant interchange-breaking terms are linear [cf. Eq. (3.10)], the system is described by the amplitude equations [4]

$$\dot{z}_+=(\mu_++i\omega_+)z_++A|z_+|^2z_++B|z_-|^2z_++C\overline{z}_+z_-^2, \tag{4.3a}$$

$$\dot{z}_-=(\mu_-+i\omega_-)z_-+A|z_-|^2z_-+B|z_+|^2z_-+C\overline{z}_-z_+^2. \tag{4.3b}$$

Here A, B, C are complex $\mathcal{O}(1)$ coefficients and the small interchange-breaking parameters $\triangle\mu\equiv\mu_+-\mu_-$, $\triangle\omega\equiv\omega_+-\omega_-$ capture the effects of a finite aspect ratio. Landsberg and Knobloch further argue that because the neutral stability curve for an unbounded system is parabolic near the minimum $\triangle\mu=\mathcal{O}(\Gamma^{-2})$ for large Γ, but anticipate that $\triangle\omega=\mathcal{O}(\Gamma^{-1})$ on the grounds that the frequency is typically not at a minimum. In this case it is possible to use averaging to eliminate the last cubic term in each equation in Eqs. (4.3), (cf. [4]). However, this simplification is only possible when $\triangle\omega\gg\triangle\mu$. In the present paper we have found, by explicit calculation, that in fact $\triangle\omega=\mathcal{O}(\Gamma^{-2})$. This result has two important consequences. First, it implies that the frequencies $\omega_\pm$ stop oscillating with Γ for large enough Γ and hence that there are no 1:1 resonances in containers of sufficiently large aspect ratio. Once this is the case all mode crossings become structurally stable with the like-parity crossings always shielded by an opposite parity instability at a lower Rayleigh number. If this is true then the structure of the neutral curves for an overstable system in a large enough container resembles that for a large aspect ratio steady state system with Neumann boundary conditions at the sidewalls, as hypothesized by Hirschberg and Knobloch [13]. This discussion suggests that, given a separation ratio S, there is an interval in Γ in which there is a substantial gap between the first two modes to set in and the next pair. This interval is larger for smaller $|S|$ but not infinite. In particular, for any S there is an aspect ratio such that, for larger Γ, the gap is absent and nonresonant crossings between modes from different families take place. Second, it indicates that no simplification of Eqs. (4.3) will take place since the frequency difference and growth rates of both modes will typically be comparable, i.e., the dynamics near the codimension-two points will be described by a pair of complex amplitude equations with broken D_4 symmetry.

It is of interest to rewrite Eqs. (4.3) in terms of traveling wave coordinates (v,w), where $z_+=v+w$, $z_-=v-w$:

$$\dot{v}=(\mu+i\omega)v+\tfrac{1}{2}(\triangle\mu+\triangle\omega)w+a|v|^2v+b|w|^2v+cw^2\overline{v}, \tag{4.4a}$$

$$\dot{w}=(\mu+i\omega)w+\tfrac{1}{2}(\triangle\mu+\triangle\omega)v+a|w|^2w+b|v|^2w+cv^2\overline{w}, \tag{4.4b}$$

where $\mu\equiv\frac{1}{2}(\mu_++\mu_-)$, $\omega=\frac{1}{2}(\omega_++\omega_-)$, and $a=A+B+C$, $b=2A-2C$, $c=A-B+C$. In this form it is possible to compare Eqs. (4.3) with the corresponding ones for an annular system in which the initial instability is a Hopf bifurcation with O(2) symmetry:

$$\dot{v}=(\mu+i\omega)v+a|v|^2v+b|w|^2v, \tag{4.5a}$$

$$\dot{w}=(\mu+i\omega)w+a|w|^2w+b|v|^2w. \tag{4.5b}$$

These equations describe the competition between traveling waves $(v,w)=(v,0)$, and standing waves $(v,w)=(v,v)$, both of which bifurcate simultaneously in such a container and have frequencies near ω. This interpretation of the amplitudes (v,w) follows from the expression for the temperature perturbation,

$$\theta(x,z,t)=\mathrm{Re}[\{ve^{ikx}+we^{-ikx}\}f(z)+\cdots], \tag{4.6}$$

where $f(z)$ is the *vertical* eigenfunction.

There are two notable differences between Eqs. (4.4) and (4.5). The first difference, the presence of the terms (w,v), is to be expected and represents the effect of breaking translation invariance at linear order; it is responsible for the splitting of the Hopf bifurcation with O(2) symmetry into two consecutive Hopf bifurcations [3]. We have seen such splitting in Fig. 5, for example. However, the second difference, the presence of the terms $(w^2\overline{v},v^2\overline{w})$ is nonperturbative and indicates that the sidewalls play an important role in the near-onset behavior of the system. Indeed, as demonstrated by Renardy [21], equations of the form (4.3) can be derived, via center manifold reduction, from a pair of coupled complex Ginzburg-Landau equations with generic boundary conditions.

ACKNOWLEDGMENTS

We are grateful to Jeff Moehlis for discussions. This work was supported by the National Science Foundation under Grant No. DMS-9703684, and by DGICYT under Grant No. PB97-0683. Computer time was provided by CEPBA.

[1] P. Kolodner, C. M. Surko, and H. Williams, Physica D **37**, 319 (1989).
[2] V. Steinberg, J. Fineberg, E. Moses, and I. Rehberg, Physica D **37**, 359 (1989).
[3] G. Dangelmayr and E. Knobloch, Nonlinearity **4**, 399 (1991).
[4] A. S. Landsberg and E. Knobloch, Phys. Rev. E **53**, 3579 (1996).
[5] D. Jacqmin and J. Heminger (unpublished) have performed similar calculations to those reported here.
[6] H. R. Z. Zangeneh, Ph.D. Thesis, University of British Columbia, 1993 (unpublished); A. S. Landsberg and E. Knobloch, Phys. Rev. E **53**, 3601 (1996).
[7] J. D. Crawford, M. Golubitsky, M. G. M. Gomes, E. Knobloch, and I. N. Stewart, Lect. Notes in Math. **1463**, 65 (1991).
[8] J. Moehlis and E. Knobloch, Phys. Rev. Lett. **80**, 5329 (1998).
[9] T. Clune and E. Knobloch, Physica D **61**, 106 (1992).
[10] T. S. Sullivan and G. Ahlers, Phys. Rev. A **38**, 3143 (1988).
[11] P. G. Daniels, Z. Angew. Math. Phys. **28**, 577 (1977).
[12] W. Nagata, Z. Angew. Math. Phys. **41**, 812 (1990).
[13] P. Hirschberg and E. Knobloch, J. Nonlinear Sci. **7**, 537 (1997).
[14] A. A. Esipov and V. Yudovich, Zh. Vychisl. Mat. Mat. Fiz. **13**, 421 (1973); **14**, 342 (1974).
[15] Y. Y. Chen, J. Fluid Mech. **241**, 549 (1992).
[16] S. A. van Gils, M. Krupa, and W. F. Langford, Nonlinearity **3**, 825 (1990).
[17] M. C. Cross, Phys. Rev. Lett. **57**, 2935 (1986); G. Dangelmayr, E. Knobloch, and M. Wegelin, Europhys. Lett. **16**, 723 (1991).
[18] E. Knobloch and D. R. Moore, Phys. Rev. A **37**, 860 (1988).
[19] I. Rehberg and G. Ahlers, Phys. Rev. Lett. **55**, 500 (1985); Contemp. Math. **56**, 277 (1986).
[20] T. S. Sullivan and G. Ahlers, Phys. Rev. Lett. **61**, 78 (1988).
[21] M. Renardy, Fluid Dyn. Res. **24**, 189 (1999).